Thermal Degradation Kinetics of Lutein, β-carotene and β-cryptoxanthin in Virgin Olive Oils.

Ramón Aparicio-Ruiz[†], Mª Isabel Mínguez-Mosquera and Beatriz Gandul-Rojas*

Chemistry and Biochemistry Pigment Group. Department of Food Biotechnology.

Instituto de la Grasa, CSIC, Avenida Padre García Tejero, 4, 41012 Sevilla, Spain.

[†], Department of Food Science & Technology. 110 Parker Food Science & Technology Bldg. 2015 Fyffe Ct. Columbus, OH 43210.

Running title: Degradation Kinetics of Lutein, β-carotene and β-cryptoxanthin in Oils.

*Corresponding author telephone: 34-954691054

telefax: 34-954691262

e-mail: gandul@cica.es

e-mail addresses of all coauthors: aparicio-ruiz.1@osu.edu

minguez@cica.es

ABSTRACT

Virgin olive oils (VOO) made with olives collected at three maturation stages were thermal degraded to determine the degradation kinetics of lutein and their isomers, β-carotene and β-cryptoxanthin. It was determined that the thermal degradative pathway of lutein occurs by competitive and parallel reactions that yield structural configuration changes (isomeriation reaction) and subsequent degradation to colorless products. While β-carotene and β-cryptoxanthin thermal degradation reaction was studied as a total degradation reaction to products. A first-order kinetic mechanism was appropriate for describing the thermal degradation of β-carotene, β-cryptoxanthin and lutein in VOO. The thermal stability varies among carotenoids and was greater for lutein than β-carotene and β-cryptoxanthin but being affected significantly by changes in their geometric configuration. A true kinetic compensation effect exists in lutein, β-carotene and β-cryptoxanthin degradation reactions.

The isokinetic study compared kinetic and thermodynamic parameters determined in the three VOO matrices of different pigment content (high, medium, and low), and found that the oily medium did not significantly affect the reaction mechanisms of any of these carotenoid compounds. Consequently, the thermodynamic parameters characterized in this study can be extrapolated to any type of VOO matrix yielding a mathematical model that predicts the carotenoid degradation and *cis*-lutein isomer formation in VOO with time, and depending on temperature. Reaction conditions similar to those used in the VOO soft deodorization process (1.5h at 120ºC) are sufficient to significantly increase the percentage of *cis*-isomers. This decreases the natural *trans*-lutein/*cis*-lutein isomer ratio between 40%-23%. Therefore, this criterion could be used to detect fraudulent use of soft deodorization in VOO.

Keywords: Virgin olive oil; carotenoids; isomerization; thermal degradation; kinetics; Arrhenius parameters; isokinetic effect, thermal stability.

1. Introduction

Carotenoids are a class of more than 600 naturally occurring pigments synthesized by plants, algae, and photosynthetic bacteria. These richly colored molecules are the sources of the yellow, orange, and red colors of many fruits and vegetables. The color is due to the presence of a chromophore in its molecule, which consists mainly or entirely of a chain of conjugated double bonds. Some carotenoids, however, have polyene chromophores that are too short to be detected by the human eye. It has been postulated that some of these substances are intermediates in the biosynthesis of other carotenoids. In plants, they are localized in subcellular organelles i.e. chloroplasts and chromoplasts. In chloroplasts, the carotenoids are mainly associated with proteins and serve as accessory pigments in photosynthesis, as photoprotective pigments, and as membrane stabilizers, whereas in chromoplasts they are deposited in crystalline form or as oily droplets (Mínguez-Mosquera et al, 2007).

Carotenoid biosynthesis occurs through the isoprenoid or terpenoid pathway. The first committing step is a head-to-head coupling of two molecules of the C_{20} geranylgeranyl diphosphate (GGDP) to yield colorless phytoene. In the following steps, the introduction of double bonds creates the light absorbing properties that determine the color of carotenoids. Besides their participation in coloring fruits and vegetables, carotenoids play an important role as functional compounds. In addition to the provitamin A value of the carotenoids with β-ionone ring, numerous epidemiological studies report that a diet rich in carotenoids is associated with a decreased risk of certain types of cancer (Maoka et al, 2001), cardiovascular disease (Rao, 2002), atherosclerosis (Kritchevsky et al, 1998) and age-related macular degeneration (AMD) (Beatty et al, 1999) and cataracts (Trumbo and Ellwood, 2006).

Carotenoids occur in nature predominantly in their all-*trans* configuration which is the thermodynamically more stable isomer (von Doering et al, 1995), while *cis*-isomers are present in small amounts, especially in chlorophyll-containing tissues. The main *cis*-isomer detected in fresh green-colored vegetables and fruits is 9-*cis*-β-carotene but 13-*cis*-isomer is found mainly in yellow and red-colored vegetables (Watanabe et al, 1999).

Research in heat processing of plant food revealed that a *trans*-*cis* isomerization of carotenoids was induced, being 13-*cis* the main isomer formed during thermal treatments while 9-*cis*-isomers were favored under illumination conditions (Pott et al, 2003; Marx et al, 2003). Since Marx et al (2003) did not find trans-*cis*-isomerization of carotene in fresh carrots, known to contain crystal-like chromoplasts, an interrelation between isomerization and alteration of crystalline carotenes by thermal processing steps was established. In particular, dissolution of carotene in oil enhanced isomerization rates significantly (Pott et al.

2003). Isomerizations and/or reactions of degradation to colorless products can modify the carotenoid biological properties such as reduce activity of provitamin A and antioxidant capacity or alter bioavailability (Schieber & Carle, 2005).

Olive oil occupies a central place in the Mediterranean diet, which has become a model example of how health can be improved through diet. Recent data suggest that its components may have a greater role in diseases prevention than previously thought. Olive oil contains a high percentage of monounsaturated fatty acids (56%-84% oleic acid) and between 3%-21% of linolenic acid, the major essential fatty acid and the most abundant polyunsaturated fatty acid in our diet. Its health claims not only stem from their adequate fatty acid composition but also other minor constituents fundamental in contributing to specific characteristics of virgin olive oil, such as its oxidative stability and its special flavor (aroma and taste) as well as its color. Among them are the phenols, chlorophyll and carotenoids, vitamin E (including α–tocopherol), β-sitosterol and squalene.

Among them, carotenoids can be emphasized. The main carotenoids in VOO are lutein and β-carotene, although there are also β-criptoxanthin and epoxidized xanthophylls such as neoxanthin, violaxanthin, antheraxanthin and their furanoid isomers (Gandul-Rojas and Mínguez-Mosquera, 1996). Along with chlorophyll compounds are the pigments responsible for the valued color of virgin olive oil. They are bioactive compounds which have provitamin A function (β-carotene and β-cryptoxanthin), antioxidant activity, and prevent age-related macular degeneration and cataract formation (lutein) (Seddon et al, 1994). The carotenoid composition of virgin olive oil is subject to wide variations due to the differences between cultivars and the degree of ripeness of the olive fruit, latitude, environmental conditions, processing techniques, and storage conditions (Gandul-Rojas and Mínguez-Mosquera, 1996; Gandul-Rojas et al, 2000; Morello et al, 2003; Salvador et al, 2003). These differences are mainly quantitative, since the qualitative composition of carotenoids is basically the same in all the olive cultivars and is not modified when the fruit is at an advanced ripening stage, its average content being between 2 and 20 mg/kg (Gandul-Rojas et al, 2000; Psomiadou and Tsimidou, 2001).

It is important to note that only virgin olive oil contains these minor compounds, since poor-quality olive oils are subject to refining processes which eliminate them, i.e. adsorption using decolorizing earth and/or deodorizing treatment at high temperatures (Usuki et al, 1984). To obtain the extra virgin grade, olive oil must satisfy the European Regulation (EC) No 2568/91 and in particular should not have sensorial defects (i.e. be rancid, musty or fusty). For this reason, soft deodorization happens to be used instead of classical deodorization, in

order to avoid the formation of stigmastadienes, which is the criterion used to detect the addition of refined oil in virgin olive oil.

The carotenoid profile of virgin olive oil can be used as a parameter of quality and authenticity for this product, since the presence of carotenoid pigments different from those just described, or the detection of a high level of carotenoid transformation is indicative of incorrect or fraudulent practices (Gandul-Rojas et al, 2000). Inadequate storage conditions with high temperatures and/or light, can cause changes in these compounds, such as isomerization or discoloration that alter both the quality of the product and their functional properties. These reactions are mainly present in deodorization treatments that olive oils with poor organoleptic quality are subjected to ("deodorized oils").

This research work is aimed at the kinetic study and characterization of the thermodynamic parameters governing the thermal degradation reactions of lutein, β-carotene and β-cryptoxanthin in VOO, to advance knowledge of the thermal resistance of these compounds in an oily matrix, and to establish mathematical models enabling the prediction of the degradation of this pigment during VOO storage and/or thermal processing.

2. Materials and methods

*2.1 Chemicals and Standards***.**

Tetrabutylammonium acetate and ammonium acetate were supplied by Fluka (Zwijndrecht, TheNetherlands). HPLC reagent grade solvents were purchased from Teknokroma (Barcelona, Spain), and analytical grade solvents were supplied by Panreac (Barcelona, Spain). For the preparation, isolation, and purification of carotenoid pigments, analytical grade reagents were used (Panreac). The deionized water used was obtained from a Milli-Q 50 system (Millipore Corp., Bedford, MA). Standard of β-carotene was supplied by Sigma Chemical Co. (St. Louis, MO). Reference sample of lutein and β-carotene was obtained from a pigment extract of fresh spinach saponified with 3.5M KOH in methanol and isolated by TLC on silica gel GF254 (0.7 mm thickness) on 20 x 20 cm plates using petroleum ether (65-95 °C)/acetone/diethylamine (10:4:1) (Mínguez-Mosquera et al., 1992). β-Cryptoxanthin was obtained from red peppers (Míguez-Mosquera and Hornero-Méndez, 1993). All standards were purified by TLC using different eluents (Mínguez-Mosquera et al., 1992).

2.2 Samples.

The study of thermal degradation of pigments was carried out with virgin olive oils obtained from a single industrial mill (Cooperativa Sor Ángela de la Cruz, Estepa, Seville) to avoid any effect of pedoclimatic and agricultural parameters and the industrial variables of the extraction systems in the comparative studies. In order to have three lots of oil with a differing pigment content, the starting material used was a mixture of two oil variety olives – Hojiblanca and Manzanilla – picked in three different months: November (sample N), December (sample D), and January (sample J). The proportion of fruits between varieties was 20/80, 80/20 and 100/0 respectively. The dates of picking correspond to high, medium, and low pigment levels (referring to the green colour) and correlated inversely with the degree of fruit ripening according to the method of Walalí-Loudiyi et al. (1984).

2.3 Heat treatment.

Preliminary assays, with a commercial sample of virgin olive oil, enabled an approximate determination of the degree of conversion for the main reactions to be studied, and established a range of times for an appropriate sampling at each temperature. The total time of each experiment changed depending on the assay temperature: 42 h (120 ºC), 64 h (100 ºC), 370 h (80 ºC) and 744 h (60 ºC). At least 128 aliquots (32 for each of the four assay temperatures)

were separated from each oil lot (samples N, D, and J). These aliquots were put into glass tubes that were sealed in the absence of air and placed in thermostatted ovens at the temperatures fixed for each experiment. These four temperatures were used to determine the kinetic and thermodynamic parameters (reaction order, reaction rate, and activation energies). For each oil lot, two samples were analysed for each time/temperature pair. The samples were removed from the thermostatted ovens at fixed time intervals, depending on each experiment, to obtain a total of at least 16 duplicate samples. The samples were cooled rapidly in an ice bath and then kept at -20 ºC until analysis of the pigments.

2.4 Extraction and Analysis of Carotenoid Pigments.

All procedures were performed under green lighting to avoid any photooxidation of carotenoid compounds. Pigment extraction was performed by liquid-phase distribution. This method was developed for virgin olive oil by Mínguez-Mosquera et al. (1990). The technique is based on the selective separation of components between N, N-dimethylformamide (DMF) and hexane. The oil sample (10-15g) was dissolved directly in 150mL of DMF and treated with five 50mL successive portions of hexane in a decanting funnel. The hexane phase carried over lipids and carotene fraction while the DMF phase retained chlorophyll pigments and xanthophylls. This system yielded a concentrated pigment solution that was oil free and could be adequately analyzed by chromatographic techniques.

The analysis of carotenoid pigments was performed according to the method described by Mínguez-Mosquera et al. (1992). β-carotene was directly quantified in hexane phase by absorbance measurement at 450nm and xanthophylls by HPLC using a reverse phased column (20cm x 0.46 cm) packed with 3 μm C18 Spherisorb ODS2 (Teknokroma, Barcelona, Spain) and an elution gradient with the solvents (A) water/ion-pair reagent/methanol (1:1:8, v/v/v) and (B) acetone/methanol (1:1 v/v), at a flow rate of 1.25 mL/min. The ion-pair reagent was 0.05M tetrabutylammonium acetate and 1M ammonium acetate in water. All-*trans*-lutein, 9-*cis*-lutein, 13-*cis*-lutein, β-cryptoxanthin and β-carotene were identified by co-chromatography with the corresponding standard and from their spectral characteristics described in detail in previous papers: wavelength absorption maxima and peak ratio III/II (Mínguez-Mosquera et al., 1992) and ratio of absorption intensity at the near-UV maximun (327-339) to the absorption intensity at the main absorption maximun for cis-isomers (Aman et al. 2005). The online UV-vis spectra were recorded from 300 to 800 nm with the photodiode array detector. Carotenoids were detected at 450 nm and were quantified from the corresponding calibrate curves (amount versus integrated peak area). The calibration

198 equations were obtained by least-squares linear regression analysis over a concentration range
199 according to the levels of these pigments in VOO. Injections in duplicate were made for five
200 different volumes at each standard solution.

201

202 *2.5 Kinetic Parameters***.** Changes in experimental data of pigment concentration, expressed in
203 µmol/kg, were used to calculate kinetic parameters by least-squares non-linear regression
204 analysis. The reaction order (n) and rate constant (k) were determined by trial and error using
205 the integral method: a reaction order is initially assumed in the rate equation and then is
206 integrated to obtain a mathematical expression that relates pigment concentration (C) with
207 time (t). The mathematical expression that best fits the changes in the experimental data with
208 the reaction time was selected to verify the order (assumed ad initio) and used to obtain the
209 rate constant (k).

210 *2.6 Thermodynamic Parameters.*

211 The effect of temperature on the rate constant was evaluated by means of the Arrhenius
212 equation with a simple reparameterization (Van Boekel., 2008) by using a reference
213 temperature T_{ref}:

214 $$k = k_{ref} \times \exp\left[\frac{-E_a}{R}\left(\frac{1}{T} - \frac{1}{T_{ref}}\right)\right]$$

215 Where R is the molar gas constant (1.98 cal mol^{-1} K^{-1}), T is the absolute temperature (K), E_a is
216 the activation energy (cal mol^{-1}), k is the specific reaction rate constant at the temperature T,
217 and k_{ref} is the specific reaction rate constant at the reference temperature T_{ref}. The reference
218 temperature should preferably be chosen in the middle of the studied temperature regimen.

219 Therefore, E_a was estimated on the basis of non-linear regression analysis of k_i *vs* $1/T_{ij}$ (being
220 i = N, D, J; j = 60 °C, 80 °C, 100 °C, 120 °C).

221 According to activate complex theory, enthalpy ($\Delta H^{\#}$) and entropy of activation ($\Delta S^{\#}$) were
222 determined by the Eyring equation:

223 $$\ln(k/T) = \frac{-\Delta H^{\#}}{RT} + \frac{\Delta S^{\#}}{R} + \ln\left(\frac{k_b}{h}\right)$$

224 Where k is the rate constant at temperature T, k_b is the Boltzmann constant; R is the molar gas
225 constant and h is the Planck constant.

Therefore, $\Delta H^{\#}$ and $\Delta S^{\#}$ were estimated on the basis of linear regression analysis of $\ln (k_i/T_{ij})$ *versus* $1/T_{ij}$. The Gibbs free energy was estimated according to the Gibbs equation:

$$\Delta G^{\#} = \Delta H^{\#} - T\Delta S^{\#}$$

The pairs of $\Delta H^{\#}$ and $\Delta S^{\#}$ obtained were linearly correlated using the last equation. From which the isokinetic temperature (T_{isok}) and its corresponding Gibbs free energy (AG_{isok}) for the reaction could be estimated

*2.7 Calculations and Statistical Data Analysis***.**

Estimated parameters were expressed as means ± SE and were analyzed for differences between means using one-way analysis of variance (ANOVA). Brown & Forsythe test (Brown & Forsythe, 1974) was used as a post hoc comparison of statistical significance (*p* values $\leq$ 0.05). Least squares and non linear regression analysis were performed using Statistica 6.0 (StatSoft, Inc., 2001) and Statgraphics Centurion XV for Windows (Statpoint Technologies, Inc., 2005).

3. Results and discussion

3.1 Kinetic study

The initial pigment content in the studied VOO matrices of high (N), medium (D), and low (J) pigmentation are shown in **Table 1**. The total pigment content includes chlorophylls and carotenoids and quantitatively is a reflection of the differences required in the starting samples, so that the effect of the pigment composition of the VOO matrix on the kinetics of thermal degradation of theses compounds can be studied (Aparicio et al, 2010). The qualitative carotenoid profile was that typical of virgin olive oil (Gandul-Rojas et al, 2000; Gandul-Rojas and Minguez-Mosquera, 1996) with lutein and β-carotene as majority carotenoids, and violaxanthin, luteoxanthin, auroxanthin, neoxanthin, antheraxanthin, mutatoxanthin and β-cryptoxanthin as minority xanthophylls.

The study of carotenoid thermal degradation in virgin olive oil has had to be separated into two sections, given the high amount of data. In the first stage of the study it will present the results for β-carotene, β-cryptoxanthin and lutein and in the next stage it will study the results concerning epoxidized xanthophylls: neoxanthin, violaxanthin, antheraxanthin and their corresponding isomers.

Figure 1 shows the typical HPLC chromatograms of an olive oil pigment extract at three significant moments of the thermal degradation process studied: initial sample and after 18 and 42 h of heating at 120ºC. In this paper we focus on lutein (peak 1), 9-*cis*-lutein (peak 2), 13-*cis*-lutein (peak 3), β-cryptoxanthin (peak 4) and β-carotene.

As the concentration of the all-*trans*-lutein gradually falls during thermal treatment, certain changes in the content of their 9-*cis* and 13-*cis*-lutein isomers were detected. Firstly, these isomers gradually increases during a given time interval until it reaches an equilibrium state at maximum concentration, which then begins to fall. This demonstrates that *cis*-isomers of lutein were also involved in degradation reactions.

The maximum concentration level for *cis*-isomers was similar for both 9-*cis* and 13-*cis* and each of them never reached more than 7% of total lutein amount. The time required to achieve this equilibrium necessarily increased with decreasing temperature, and in all cases higher values for the 9-*cis* isomer were maintained for all temperatures and matrices studied. At 120ºC, 13-*cis* isomer reached its maximum content at 6-9 h of heat treatment, when lutein retention was 72%, while 18 h of treatment was necessary for 9-*cis* isomer concentration, when lutein retention drops to 55%. In any case, after an hour and half of heat treatment at 120ºC, similar to that used in VOO soft deodorization, reaction conditions were presented

which were sufficient to significantly increase the percentage of *cis*-isomers, decreasing significantly the natural *trans* lutein/*cis*-lutein isomers ratio between 40%-23%. This criterion could therefore be used to detect fraudulent use of soft deodorization in VOO.

Similarly to that of lutein, β-carotene undergoes *cis*-isomerization after heat treatment (Achir et al, 2010). A recently published study showed a kinetic model for β-carotene isomerization in a real food system using carrot puree. Changes in the extractability of β-carotene induced by heat treatment meant that reactions of oxidative degradation could not be considered for uncolored products (Lemmens et al, 2010). In our study the analytical conditions used have prevented an individual quantification of those isomers. As detailed in the methods section, during the extraction of pigments from VOO matrix by liquid-phase distribution, the β-carotene is retained in the hexane phase with the lipid fraction and it was directly quantified by absorbance measurement at 450nm. Thus, the only change observed for β-carotene and β-cryptoxanthin was that they disappeared during the heat treatment. Accordingly, an identical kinetic mechanism was proposed for β-carotene and β-cryptoxanthin. In simplified form, a one-step reaction was considered (**Figure 2**), in which the reagents (β-carotene and β-cryptoxanthin) give rise to colorless products, regardless of the reaction intermediate pathways. In accordance with these mechanisms, the corresponding kinetic equations are expressed as:

$$V_{\beta-\text{Carotene}} = -\frac{d[A]}{dt} = k_1[A]^n \qquad [1]$$

$$V_{\beta-\text{Cryptoxanthin}} = -\frac{d[C]}{dt} = k_2[C]^n \qquad [2]$$

where [A] and [C] are the concentration of β-carotene and β-cryptoxanthin respectively, [B] and [D] the concentration of colorless degradation products, k_1 and k_2 the rate constants for the respective reactions and n is the reaction order.

Resolving the kinetic model, assuming an order of 1 (n=1) and that all reactions are irreversible, we obtain:

$$[A] = [A]_0 e^{-k1 \cdot t} \qquad [3]$$

$$[C] = [C]_0 e^{-k2 \cdot t} \qquad [4]$$

The individual quantification of different *cis*-lutein isomers allowed us to propose a more complex kinetic mechanism for the lutein degradation to colorless products (**Figure 3**) than the previous one. The thermal degradation of lutein involves two parallel reactions for the formation of 9-*cis*-lutein and 13-*cis*-lutein and a third reaction of oxidative degradation of

the chromophore. It also includes two consecutive reactions from 9-*cis*-lutein and 13-*cis*-lutein leading to colorless products. In line with this mechanism proposed, the corresponding kinetic equations are expresed as:

$$V_{lutein} = -\frac{d[A]}{dt} = k_{tc}[A]^n \text{ ; where } k_{tc} = k3 + k5 + k7 \quad [5]$$

$$V_{9-cis-lutein} = \frac{d[B]}{dt} = k_3[A]^n - k_4[B]^n \quad [6]$$

$$V_{13-cis-lutein} = \frac{d[C]}{dt} = k_5[A]^n - k_6[C]^n \quad [7]$$

$$V_{nc} = \frac{d[D]}{dt} = k_7[A]^n + k_4[B]^n + k_6[C]^n \quad [8]$$

where: [A] is the all-*trans*-lutein concentration; [B] is the 9-*cis*-lutein concentration; [C] is the 13-*cis*-lutein concentration; [D] is the concentration of colorless products (nc); k_3, k_4, k_5, k_6, and k_7, are the rate constants for the different reactions; and n is the reaction order.

Using the material balance of all species, the next equation allows us to obtain the concentration of colorless products with time:

$[A]_0 + [B]_0 + [C]_0 + [D]_0 = [A] + [B] + [C] + [D]$.

Here $[A]_0$ is the initial concentration of all-*trans*-lutein; $[B]_0$ is initial concentration of 9-*cis*-lutein; $[C]_0$ is initial concentration of 13-*cis*-lutein; $[D]_0$ initial concentration of colorless products; and [A]-[D] are those described for equations 5-8.

Resolving the kinetic model, assuming an order of 1 (n=1) and that all of the reactions are irreversible, we obtain:

$$[A] = [A]_0 e^{-k_{tc} \cdot t} \quad [9]$$

$$[B] = \frac{k_3[A]_0}{k_4 - k_{tc}}\left[e^{-k_{tc} \cdot t} - e^{-k_4 \cdot t}\right] + [B]_0 e^{-k_4 \cdot t} \quad [10]$$

$$[C] = \frac{k_5[A]_0}{k_6 - k_{tc}}\left[e^{-k_{tc} \cdot t} - e^{-k_6 \cdot t}\right] + [C]_0 e^{-k_6 \cdot t} \quad [11]$$

In accordance with the proposed kinetics equations 3, 4, 9-11 and by nonlinear regression analysis of the experimental data, the rate constants for each of the proposed reactions in the mechanisms (**Figures 2** and **3**) were estimated. For the treatment at 120ºC of the high-pigmentation matrix (sample N) **Figures 4** and **5** exemplify, the concentration changes found and the regression estimated. **Table 2** shows the values for the estimated rate constants, together with their standard error and the determination coefficient (R^2) for each reaction studied.

The determination coefficients obtained indicated a good fit of the experimental data to the equations proposed and demonstrate that the first-order mechanism is appropriate for describing the thermal degradation of β-carotene, β-cryptoxanthin and lutein in VOO. Studies describing the kinetics of carotenoids in fruit- and vegetable-based products are rather limited although this information would be very useful and industrially relevant for predicting nutritional changes during fruit and vegetable processing (Lemmens et al, 2010). In those studies, analysis of kinetic data also suggested a first-order model to describe thermal degradation of carotenoids in paprika oleoresins (Pérez-Gálvez et al, 2000), citrus juice (Dhuique-Mayer et al, 2007), carrot puree (Lemmens et al, 2010) and oils enriched with β-carotene and lutein (Achir et al, 2010).

In general, all kinetic constants tripled for each 20ºC increase in temperature, demonstrating a marked effect of temperature in reaction rates. However, this effect was lower than that found in the thermal degradation of chlorophyll compounds in VOO (Aparicio et al, 2010).

The rate constant estimated for total lutein degradation was slightly lower than that of β-carotene and β-cryptoxanthin in all temperatures and matrices, suggesting that lutein has a relatively greater heat resistance, a result which agrees with other studies by Henry et al (1998) and Achir et al (2010) in oil model systems.

Geometric configuration significantly affected the thermal stability. 13-*cis*-lutein was the most labile isomer, with greater degradation rate constants than those for 9-*cis* at all temperatures. The k for the isomer formation was always about 10-15 times lower than the k of degradation in all cases, indicating that isomer degradation is the preferred reaction. With regard to the isomer type, significantly higher values were found for 13-*cis* isomer formation rate constants. This result is consistent with other studies by Updike and Schwartz (2003) who quantified the percentage of lutein and zeaxanthin isomerization in thermally processed vegetables showing a predominant formation of isomer 13-*cis* lutein.

According to the kinetic mechanism propounded for the lutein degradation (**Figure 3**), the sum of constants k_3, k_5, and k_7 should be equal to k_{tc} (kinetic constant of the total degradation of lutein). Differences between $k_3 + k_5$ and k_{tc} were analyzed by ANOVA (t-test $P \leq 0.05$) and the results are shown in **Table 3**. In most cases no significant difference was found between these parameters, allowing k_7 to be ignored, i.e., ruling out the hypothesis in the kinetic mechanism that colorless products are formed directly from *trans*-lutein. This reaction either does not happen or is very slow compared to the two *cis*-isomerization reactions that take place simultaneously.

3.2 Thermodynamic study

The Arrhenius model and transition state theory were used to determine the influence of temperature on the reaction rates. **Table 4** displays the values estimated for the thermodynamic parameters (entropy, enthalpy, activation energy and Gibbs free energy), with their respective standards errors for each matrix and reaction analyzed.

To study the effect of the type of matrix on the reaction mechanism, we compared the thermodynamic parameters estimated in the three types of VOO. No significant differences were found in the parameters $\Delta S^{\#}$ and $\Delta H^{\#}$ characterizing the reaction of total degradation of lutein and the reactions of formation and degradation of 9-*cis* and 13-*cis*-lutein (t-test $P \leq 0.05$) (**Table 4**). These results enable all of the matrices to be considered a single reaction medium. Significant differences in the thermodynamic parameters corresponding to degradation reaction of β-cryptoxanthin and β-carotene were found in matrix J suggesting in this case a slight effect of the matrix.

With respect to the estimated values for activation energy of isomerization reactions of lutein, higher values were found in 13-*cis*-lutein isomer formation, in all matrices studied. Mathematically, the interpretation is that a temperature increase produces a greater increase in the rate constant for 13-*cis* isomer formation, i.e. this reaction would be preferred. By comparing matrices, the values of E_a were significantly higher in the matrix N, for the reactions of both *cis* isomers formations. In addition to factors such as light and heat, the presence of other components with antioxidant capacity can influence these reactions by partially inhibiting isomerization and degrading carotenoids (Schieber and Carle, 2005). α-tocopherol and pheophytins also have this capability. They are present in VOO and are higher in content at the beginning of the harvesting season (matrix N).

Higher activation energy of lutein as compared to β-cryptoxanthin and β-carotene implies that a smaller temperature change is needed to degrade lutein more rapidly.

In all cases, $T\Delta S^{\#}$ values were always negative; however, enthalpy values ($\Delta H^{\#}$) were always positive, as were the Gibbs free energy values ($\Delta G^{\#}$), making the reactions nonspontaneous.

3.3 Isokinetic ratio

Isokinetic ratio was studied in the same lines as a previous study (Aparicio-Ruiz et al, 2010), so as to determinate whether there are changes in the reaction mechanisms or greater importance of some specific step of the mechanism under our different experimental conditions (VOO matrices with high, medium and low pigmentation).

The isokinetic effect (or isoequilibrium) has to be defined as the existence of an intersection point between the straight Arrhenius lines (or van't Hoff) that show the thermodynamics of a series of similar reactions or a reaction in different media (Karpinski and Larsson, 1997). This cutoff point is the isokinetic temperature at which the reactions take place at identical rates. Specifically, the experiments study the same reaction taking place in different oily matrices. We thus find ourselves in the second case: a greater importance of a particular step of the mechanism. To study the existence of the isokinetic ratio between the oily matrices, the Arrhenius straight lines obtained for each of the three oily matrices studied were represented together. The study was repeated for each of the reactions including the mechanism of thermal degradation of lutein, β-cryptoxanthin and β-carotene; no isokinetic ratio was found for any of them.

For example, in total lutein degradation reaction (**Figure 6**), we could not conclude that there was an isokinetic ratio as the Arrhenius straight lines for the three samples (N, D, J) did not present any common cut-off points. These straight lines are almost parallel, but are also very close to one another (all the points lie within the same interval of confidence). They are, therefore, isoenthalpic and isoentropic straight lines. This observation is coherent with the thermodynamic parameters (**Table 5**), which do not show significant differences (t-test $P \leq 0.05$) between the different oily matrices. Thus, there is no isokinetic ratio, and it can be concluded that the type of oily matrix does not affect the mechanism of the reactions of lutein, β-cryptoxanthin and β-carotene degradation during any of its steps. Consequently, the thermodynamic parameters characterized here can be extrapolated to any type of VOO matrix.

The isokinetic effect can also be considered in a series of similar reactions as in the case of the isomerization of lutein to form the 9- or 13-*cis* isomers, or the degradation of 9-*cis* and 13-*cis* isomers to form colorless products, and degradation of lutein, β-cryptoxanthin and β-carotene to colorless products. The average values of the rate constants obtained in the three VOO matrices studied were used to obtain the Arrhenius straight lines (**Figure 7** and **Figure 8**). In the first and the second case (**Figure 7** upper and lower, respectively), there is a cut-off point where the Arrhenius straight lines intersect. This point (isokinetic temperature) is estimated at 391 K (≈118°C) and 423 K (≈150°C), respectively. The first result indicated the same isomerization mechanism for both isomers but is affected, in one or another of its steps, by the temperature change. Thus, at temperatures above the isokinetic temperature, this reaction is quicker in 13-*cis* isomerization, and below that temperature there will be predilection for 9-*cis* lutein. In the second case the opposite occurs: at temperatures above the isokinetic temperature, this reaction is quicker in 9-*cis* degradation reaction and below that

435 temperature there will be a preference for for 13-*cis* lutein degradation reaction. However, for
436 the third case (**Figure 8**) no isokinetic ratio was found as the Arrhenius straight lines for the
437 three degradation reactions did not present any common cut-off points. These straight lines
438 are isoenthalpic and isoentropic straight lines, given that they are almost parallel, but are also
439 very close to one another (all the points lie within the same interval of confidence).
440
441 ***3.3 Compensation Effect***
442 Liu and Guo (2001) have demonstrated that the compensation effect and the isokinetic effect
443 are not necessarily synonymous as had been considered historically and that the existence of
444 one does not imply the existence of the other. A kinetically compensated system requires that
445 the different thermodynamic parameters obtained for the same reaction in different
446 environments define an isokinetic line. This theoretical line includes all of the different kinetic
447 and thermodynamic coordinates of a single reaction: with the isokinetic temperature (T_{iso})
448 being the line slope and the increase in Gibbs free energy of all reactions at the T_{iso} the
449 intercept, according to:
450 $\Delta H^{\#} = T_{iso}\Delta S^{\#} + \Delta G^{\#}$
451 Errors are inevitable in experiments and the data used are therefore estimators of the
452 corresponding variables. Consequently, it is possible that the real values are not correlated,
453 although their estimators are. This would be the case in the so-called false compensation
454 effect. Krug et al (1976) propose that the straight line in the plane ΔH versus ΔS is only a
455 manifestation of the statistical pattern of the compensation, and this hypothesis can be ruled
456 out if the estimation of the line slope is sufficiently different from the harmonic temperature
457 (T_{hm}), defined as:
458 $$T_{hm} = \frac{n}{\sum_{i=1}^{n} \frac{1}{T_i}}$$
459 Liu and Guo (2001) have proposed a method for distinguishing the real compensation
460 effects from the false ones, based on a graphical representation of the experimental values of
461 enthalpies and entropies with their error bars in the plane $\Delta H^{\#}$ versus $\Delta S^{\#}$.
462 To apply this study to our experimental data the linear regressions $AH^{\#}$ versus $AS^{\#}$ has
463 been estimated for each of the reactions. **Table 5** shows the values obtained for the line slope
464 (T_{iso}) and the corresponding determination coefficients (R^2). An isokinetic line was obtained
465 in all cases (R^2>0.95) (except in 13-*cis* lutein formation and 9-*cis*-lutein degradation).

However, by comparing the estimated isokinetic temperature and the T_{hm} under the study conditions (362 K), it is deduced that the compensation effect can only be true for the series of similar reactions that involved formation of *cis*-isomerization of lutein, degradation of 9-*cis* and 13-*cis*-lutein to colorless products and degradation reactions to colorless products (degradation of lutein, β-carotene and β-cryptoxanthin). Finally, application of the method of error bars proposed by Liu and Guo (2001) shows a true compensation effect in the case of degradation of lutein, β-carotene and β-cryptoxanthin (**Figure 9**).

4. Conclusions

The degradation of β-carotene, β-cryptoxanthin and lutein followed first-order kinetics in VOO during heat treatment. The analysis of the reaction intermediates that appear during the thermal degradation of lutein to colorless products has established that the degradation process is not simple, but takes place in several competitive elemental steps that yield structural configuration changes (isomerization reaction) and subsequent degradation to colorless products. The thermal stability varied among carotenoids and was greater for lutein than β-carotene and β-cryptoxanthin but being affected significantly by changes in their geometric configuration. No significant effect of the oily medium on the reaction mechanisms of any of these carotenoid compounds have been found from the isokinetic study, which compared kinetic and thermodynamic parameters determined in the three VOO matrices of different pigment content (high, medium, and low). The thermodynamic parameters characterized in this study could therefore be applied to any type of VOO matrix yielding a mathematical model developed from activation energies, which predict carotenoid degradation and *cis*-lutein isomer formation if the time–temperature profile of that processing method is known. Reaction conditions similar to those used in the soft deodorization of VOO (1.5h at 120ºC) are sufficient to significantly increase the percentage of *cis*-isomers, decreasing the natural *trans*-lutein/*cis*-lutein isomer ratio between 40%-23%. This criterion could therefore be used to detect fraudulent use of soft deodorization in VOO.

Acknowledgment

We thank Sergio Alcañiz-García for his technical assistance.

This work was supported by the Comisión Interministerial de Ciencia y Tecnología (CICYT-EU, Spanish and European Government) and FEDER (CE) in the Project AGL-2007-66139-C02-01 and by the Junta de Andalucía (AGR 148-2008-9).

LITERATURE CITED

Achir N., Randrianatoandro V.A., Bohuon P., Laffargue A., Avallone S. (2010). Kinetic study of beta-carotene and lutein degradation in oils during heat treatment. *Eur. J. Lipid Sci. Technol. 112*, 349-361.

Aman R., Biehl J., Carle R., Conrad J., Beifuss U., Schieber A. (2005) Application of HPLC coupled with DAD, APcI-MS and NMR to the analysis of lutein and zeaxanthin stereoisomers in thermally processed vegetables. *Food Chem. 92*, 753-763.

Aparicio-Ruiz, R., Mínguez-Mosquera, M.I., Gandul-Rojas, B. (2010). Thermal Degradation Kinetics of Chlorophyll Pigments in Virgin Olive Oils. 1. Compounds of Series *a*. *J Agric Food Chem., 58*, 6200-6208.

Beatty, S., Boulton, M., Koh, H.-H., & Murray, I. J. (1999). Macular pigment and age relatedmacular degeneration. *British Journal of Ophthalmology, 83*, 867–877.

Bermúdez B., Pacheco Y., López S., Abia R., Muriana J.G. (2004). Digestion and absoption of olive oil. *Grasas y Aceites 55* (1): 1-10.

Brown M.B., Forsythe A.B. (1974). Robust tests for the equality of variances, *J. Am. Statistical Assoc. 69*, 364–367.

Dhuique-Mayer C., Tbatou M., Carail M., Caris-Veyrat C., Dornier M., & Amiot MJ. (2007). Thermal degradation of antioxidant micronutrients in Citrus juice: Kinetics and newly formed compounds. *J. Agric. Food Chem. 55*, 4209-4216.

Gandul-Rojas, B., Mínguez-Mosquera, M.I. (1996). Chlorophyll and carotenoid composition in virgin olive oils from various spanish olive varieties. *J. Sci. Food Agric. 72*, 31-39.

Gandul-Rojas, B., Roca-L.Cepero, M., Mínguez-Mosquera, M.I. (2000). Use of chlorophyll and carotenoid pigment composition to determine authenticity of virgin olive oil. *J. Am. Oil. Chem. Soc. 77*, 853-858.

Henry L.K., Catignani G., & Schwartz S., (1998), Oxidative degradation kinetics of lycopene, lutein, and 9-cis and all-trans beta-carotene. *J. Am. Oil Chem. Soc. 75*, 823-829.

Hornero-Méndez D., Gandul-Rojas B., Mínguez-Mosquera M.I. (2005). Routine and sensitive SPE-HPLC method for quantitative determination of pheophytin *a* and pyropheophytin *a* in olive oils. *Food Research Int. 38*, 1067-1072.

Karpinski, Z.; Larsson, R. (1997) On the isokinetic effect of neopentane hydrogenolysis over metal catalysts. *J. Catal*., 168, 532-537.

Krug, R.R., Hunter, W.G., Grieger, R.A., (1976). Enthalpy-entropy compensation: 1.Some fundamental statistical problems associated with the analysis of Van't Hoff and Arrenhius data. 2. Separation of the chemical from the statistical effect. *J. Physical Chem*. *80,* 2335-2351.

Liu, L., Guo, Q.X., (2001). Isokinetic Relationship, Isoequilibrium Relationship, and Enthalpy-Entropy Compensation. *Chem. Rev. 101,* 673-695.

Kritchevsky, S. B., Tell, G. S., Shimakawa, T., Dennis, B., Li, R., Kohlmeier, L., Steere, E., & Heiss, G. (1998). Provitamin A carotenoids intake and carotid artery plaques: the atherosclerosis risk in communities study. *Am J Clin Nutr, 68,* 726–733.

Lemmens L., De Vleeschouwer K., Moelants K.R.N., Colle I.J.P., Van Loey A.M., Hendrickx M.E., (2010), Beta-Carotene Isomerization Kinetics during Thermal Treatments of Carrot Puree. *J. Agric. Food Chem. 58,* 6816-6824**.**

Maoka, T., Mochida, K., Kozuka, M., Ito, Y., Fujiwara, Y., Hashimoto, K., Enjo, F., Ogata, M., Nobukuni, Y., Tokuda, H., Nishino, H. (2001). Cancer chemopreventive activity of carotenoids in the fruits of red paprika *Capsicum annuum* L. *Cancer Lett., 172,* 103-109.

Marx, M., Schieber, A., Carle, R. (2003). Effects of thermal processing on *trans*-*cis*-isomerization of *β*-carotene in carrot juices and carotene-containing preparations. *Food Chem. 83,* 609-617.

Mínguez-Mosquera, M.I., Gandul-Rojas, B., Gallardo-Guerrero, L. (1992). Rapid method of quantification of chlorophylls and carotenoids in virgin olive oil by HPLC. *J. Agric. Food Chem*. *40,* 60-63.

Mínguez-Mosquera, M.I., Gandul-Rojas, B., Garrido-Fernández, J., Gallardo-Guerrero, L. (1990). Pigments present in virgin olive oil. *J. Am. Oil. Chem. Soc*. *67,* 192-196.

Mínguez-Mosquera, M. I.; Hornero-Méndez, D. (1993) Separation and quantification of the carotenoid pigments in red peppers (*Capsicum annuum* L.), paprika and oleoresin by reversedphase HPLC. *J. Agric. Food Chem. 41,* 1616-1620.

Mínguez-Mosquera, M.I.; Hornero-Méndez, D. & Pérez-Gálvez, A. (2007). Analysis of carotenoids and provitamin A in functional foods. In: Hurst, W.J. (Ed)(2nd edition), Methods of analysis in funtional foods and added nutraceuticals (pp 277-335).CRC Press LLC Boca Raton, FL, USA.

Morello J.R., Motilva M.J., Ramo T., Romero M.P., (2003). Effect of freeze injuries in olive fruit on virgin olive oil composition. *Food Chem. 81,* 547-553.

Pérez-Gálvez, A., Jarén-Galán, M. and Mínguez-Mosquera, M.I., (2000). Effect of high-temperature degradative processes on ketocarotenoids present in paprika oleoresins. *J. Agric. Food Chem. 48,* 2966-2971.

Pott, I., Marx, M., Neidhart, S., Mühlbauer, W., Carle, R. (2003). Quantitative determination of *β*-carotene stereoisomers in fresh, dried, and solar dried mangoes (*Mangifera indica* L.). *J. Agric. Food Chem. 51*, 4527-4531.

Psomiadou E., Tsimidou M., (2001). Pigments in Greek virgin olive oils: occurrence and levels. *J. Sci. Food Agric. 81*, 640-647.

Rao, A.V. (2002). Lycopene, tomatoes, and the prevention of coronary heart disease. *Exp Biol Med., 227,* 908-913.

Salvador M.D., Aranda F., Gomez-Alonso S., Fregapane G., (2003). Influence of extraction system, production year and area on Cornicabra virgin olive oil: a study of five crop seasons. *Food Chem. 80*: 359-366.

Schieber, A., Carle, R. (2005). Occurrence of carotenoid *cis*-isomers in food: Technological, analytical and nutritional implications. *Trends Food Sci. Technol. 16*, 416-422.

Seddon J.M., Ajani U.A., Sperduto R.D., Hiller R., Blair N., Burton T.C., Farber M.D., Gragoudas E.S., Haller J., Miller D.T., Yannuzzi L.A., Willett W. (1994) Dietary carotenoids, vitamin-A, vitamin-C, and vitamin-E, and advanced age-related macular degeneration. *JAMA 272*, 1413-1420.

Trumbo, P.R., Ellwood, K.C. (2006). Lutein and zeaxanthin intakes and risk of age-related macular degeneration and cataracts: an evaluation using the Food and Drug Administration's evidence based review system for health claims. *Am J Clin Nutr, 84*, 971-974.

Updike A.A., Schwartz S.J., (2003). Thermal processing of vegetables increases cis isomers of lutein and zeaxanthin**.** *J. Agric. Food Chem. 51*, 6184-6190**.**

Usuki R., Suzuki T., Endo Y., and Kaneda T., (1984). Residual amounts of chlorophylls and pheophytins in refined edible oils. *J. Am. Oil Chem Soc. 61*, 785-788.

Van Boekel M.A.J.S. (2008). Kinetic Modeling of Food Quality: A Critical Review. *Comprehen Rev. Food Sci & Food Safe. 7*, 144-158.

von Doering, W. E., Sotiriou-Leventis, C., Roth, W. R. (1995). Thermal interconversions among 15-*cis*-, 13-*cis*-, and all-*trans*-*β*-carotene: Kinetics, Arrhenius parameters, thermochemistry, and potential relevance to anticarcinogenity of all-*trans*-*β*-carotene. *J. Am. Chem. Soc. 117*, 2747-2757.

Walalí-Loudiyi, D., Chimitah, M., Loussert, R., Mahhou, A., Boulouha, B. (1984). Morphologic and physiologic characters of olive chlones from Picholine Marroqui variety. *Olivae, 3*, 26-31.

Watanabe, K., Kon, M., Takahashi, B., Hirota, S. (1999). *Cis-trans* isomers of *β*-carotene in fresh vegetables and fruits. *Food Sci. Technol. Res. 5*, 308-310.

FIGURE CAPTIONS

Figure 1. HPLC profile of carotenoid pigments from virgin olive oils (sample N), at initial time (0 h) and after 18 and 42 h of thermal treatment at 120 ºC. Detection was by absorption at 450nm. Peaks: 1, All-*trans*-lutein; 2, 9-*cis*-lutein; 3, 13-*cis*-lutein; 4, β-cryptoxanthin. **Figure 2.** Kinetic mechanisms for thermal degradation reaction of β-carotene and β-cryptoxanthin in virgin olive oil.

Figure 3. Kinetic mechanisms for thermal degradation pathway of all-*trans*-lutein in virgin olive oil.

Figure 4. Evolution of concentration-time of β-carotene ( ) and β-cryptoxanthin ( ) in virgin olive oil (sample N) during 42 h at 120 ºC, and corresponding fits ( ) to the mathematical model developed in this study (equations 3-4).

Figure 5. Evolution of concentration-time of all-*trans*-lutein ( ), 9-*cis*-lutein ( ) and 13-*cis*-lutein ( ) in virgin olive oil (sample N) during 42 h at 120 ºC, and corresponding fits ( ) to the mathematical model developed in this study (equations 9-11).

Figure 6. Arrhenius plot for the degradation of all-*trans*-Lutein in virgin olive oil samples studied (N, ; D, ; J,). Confidence intervals (95%).

Figure 7. Arrhenius plot for 9-*cis*-lutein ( ) and 13-*cis*-lutein ( ) formation (upper) and degradation (lower) in virgin olive oil. Average values from the three samples (N, D, J). Confidence intervals (95%).

Figure 8. Arrhenius plot for a series of similar reactions: β-carotene (○), β-cryptoxanthin (□) and all-*trans*-Lutein ( ) degradation in virgin olive oil. Average values from the three samples (N, D, J). Confidence intervals (95%).

Figure 9. Graphic representation of $AH^{\#}$ versus $AS^{\#}$ by error bars method (Liu and Guo, 2001) for a true compensation effect in the degradation of β-carotene, β-cryptoxanthin and *all-trans*-lutein to noncoloured products.

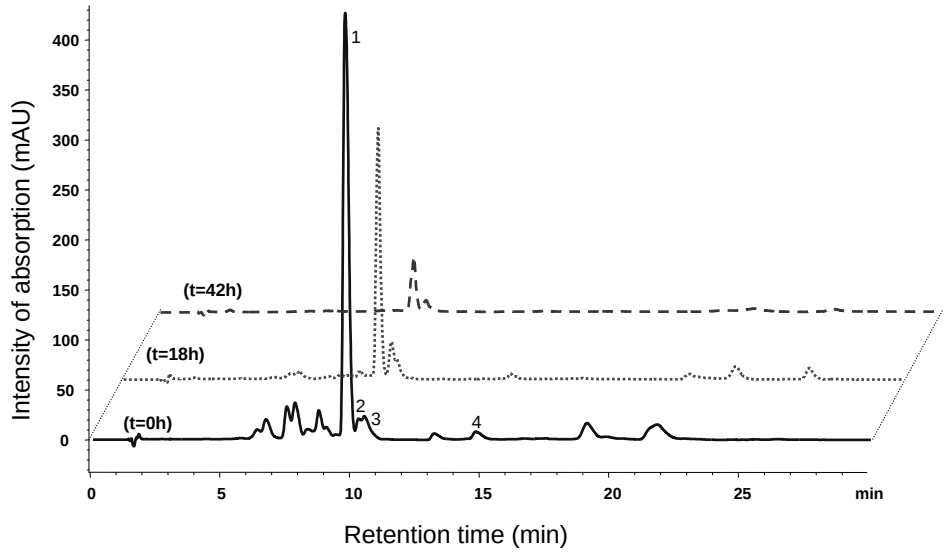

Figure 1

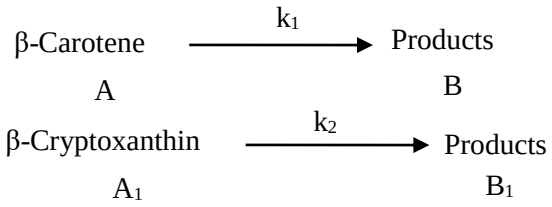

Figure 2

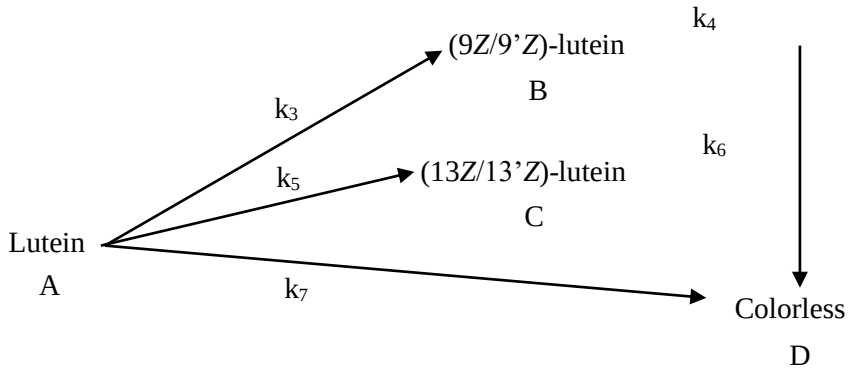

Figure 3

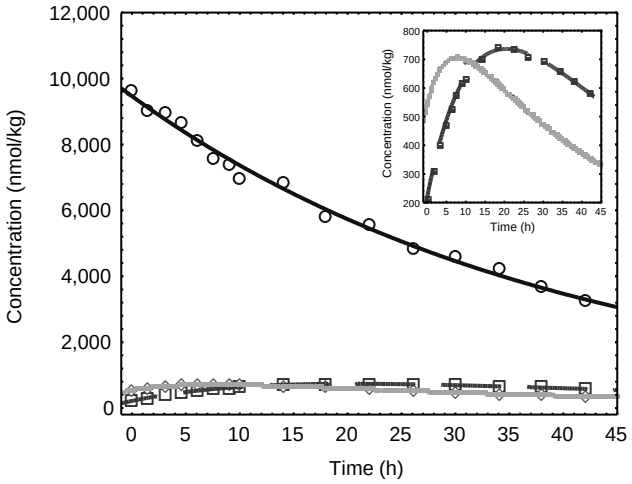

Figure 4

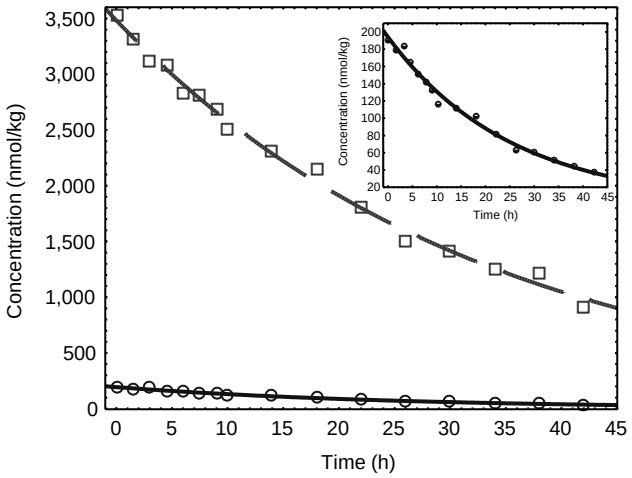

Figure 5

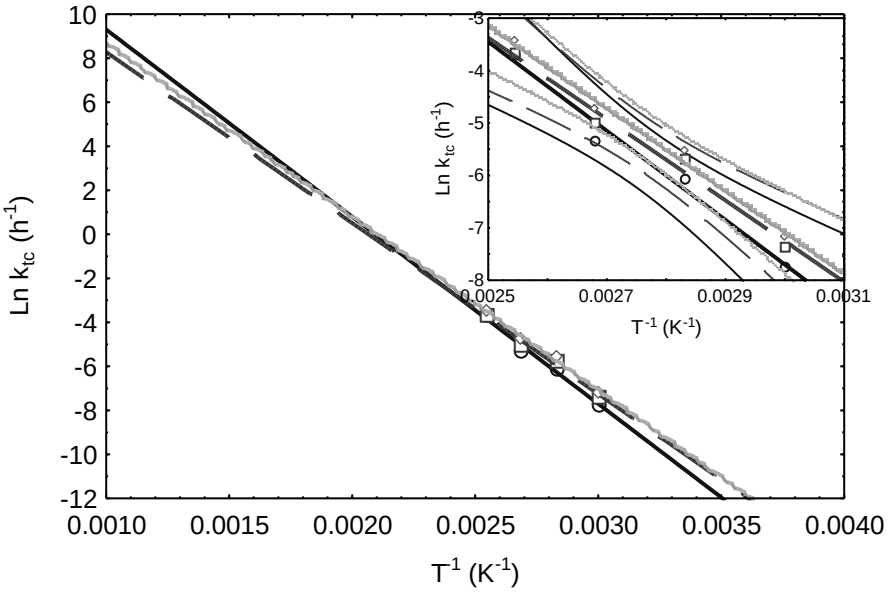

Figure 6

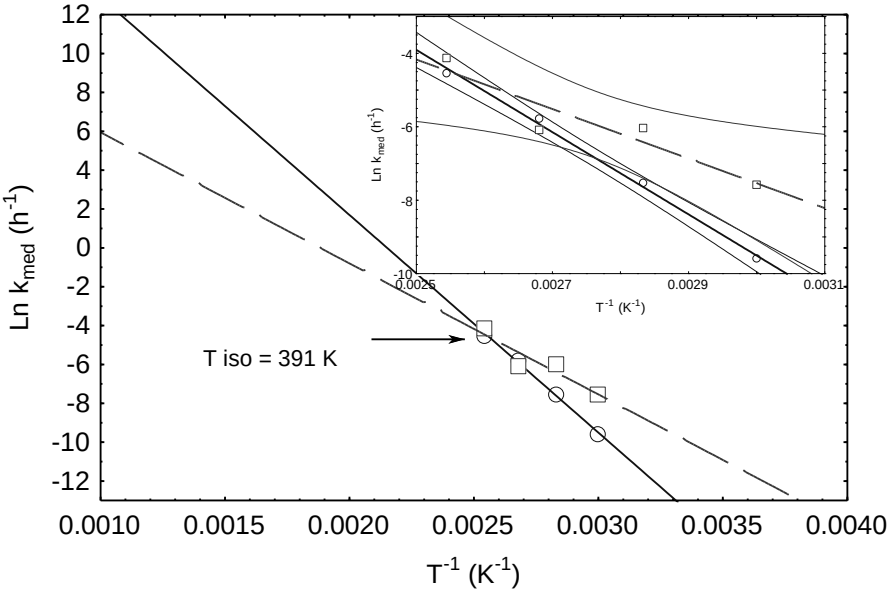

Figure 7

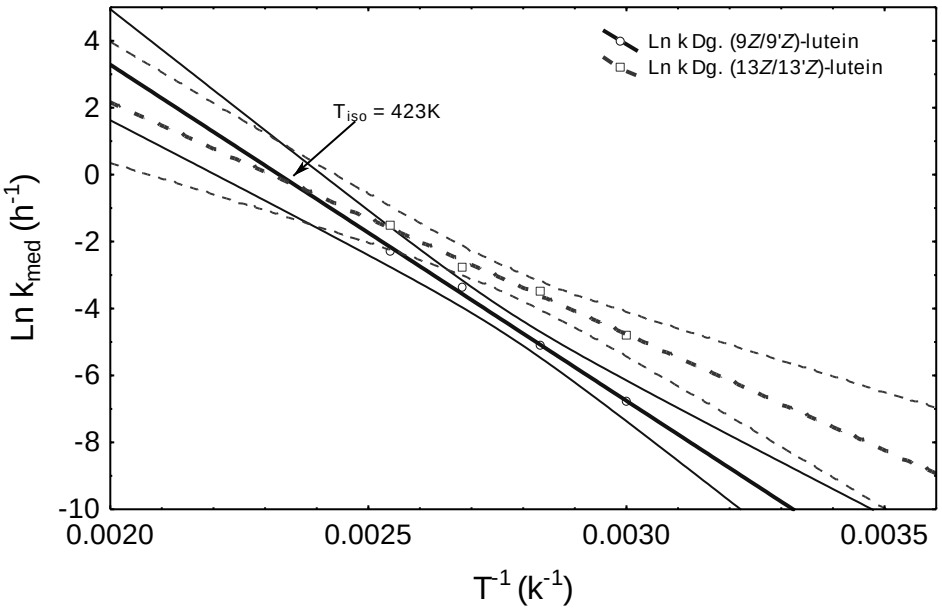

Figure 8.

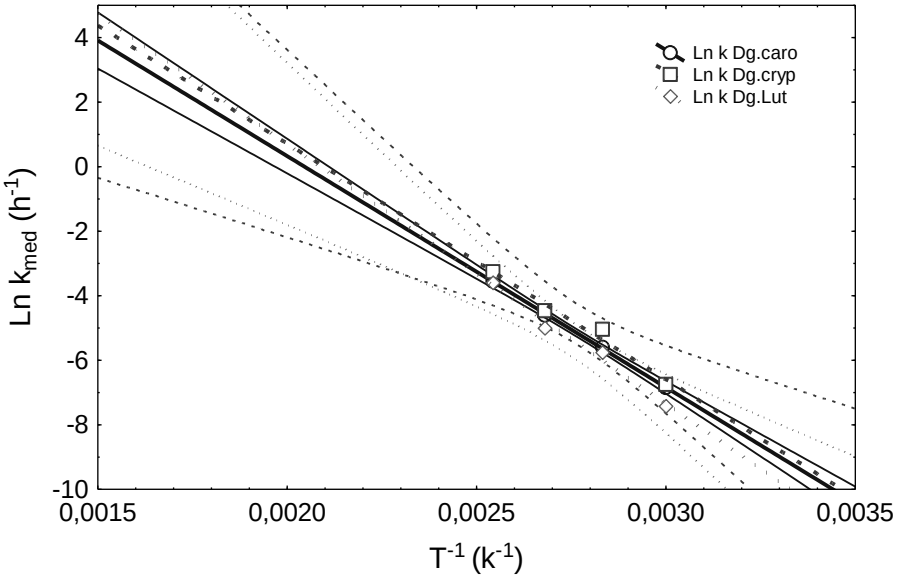

Figure 9.

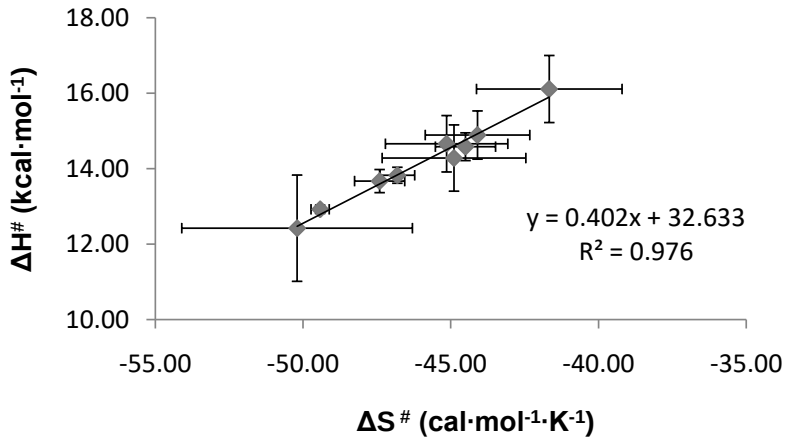
18.00
16.00
14.00
12.00
10.00
ΔH# (kcal·mol-1)
y = 0.402x + 32.633
R² = 0.976
-55.00
-50.00
-45.00
-40.00
-35.00
ΔS # (cal·mol-1·K-1)

Figure 10.

Table 1. Initial Content for Carotenoid Compounds and Total Pigments in Virgin Olive Oils[a].

Sample[b]	Lutein	(9Z/9'Z)-lutein	(13Z/13'Z)-lutein	β-carotene	β-cryptoxanthin	Total Pigments[c]
N	9.625±0.342	0.217±0.000	0.547±0.001	3.523±0.053	0.192±0.002	32.031±0.484
D	11.517±0.470	0.390±0.017	0.327±0.002	2.880±0.028	0.127±0.001	25.264±0.825
J	9.468±0.192	0.268±0.001	0.237±0.004	0.970±0.037	0.056±0.000	14.441±0.251

[a] Data, expressed as μmol/kg, represent mean values ± SD for three determinations. CV≤4.5%.
[b] The sample codex corresponds to the harvesting date of the olive fruits used to obtain the virgin olive oils studied, November (N), December (D), January (J).
[c] Total of chlorophyll and carotenoid pigments.

Table 2. Rate Constants (k) and Determination Coefficients (R^2) Estimated for the Kinetic Mechanism for the Thermal Degradation of Lutein, β-carotene and β-cryptoxanthin in VOO.

		120ºC		100ºC		80ºC		60ºC	
Reaction[a]	**S[b]**	**(k±SE)[c] x 10^3(h^{-1})**	**R^2**	**(k±SE)[c] x 10^3(h^{-1})**	**R^2**	**(k±SE)[c] x 10^3(h^{-1})**	**R^2**	**(k±SE)[c] x 10^3(h^{-1})**	**R^2**
D. Lutein	N	25.44±1.11 a	0.975	4.94±0.25 a	0.934	2.36±0.13 a	0.969	0.44±0.02 a	0.963
k_{tc}	D	25.70±1.68 a	0.949	6.87±0.36 b	0.935	3.40±0.12 b,e	0.985	0.64±0.03 b,c	0.959
	J	32.17±1.38 b,c	0.976	8.78±0.29 c,e,r	0.975	3.98±0.14 c,d	0.986	0.77±0.72 c,d-p	0.972
D. β-carotene	N	29.87±0.73 c	0.994	11.32±0.34 d,g	0.989	4.02±0.10 d	0.996	1.03±0.02 d,k	0.995
k_1	D	29.70±0.75 c	0.994	9.12±0.29 e	0.987	3.49±0.10 e	0.994	1.02±0.03 d,k	0.992
	J	26.97±0.69 d,a	0.993	9.80±0.21 f	0.994	3.62±0.10 e	0.995	1.14±0.04 e,m	0.986
D. β-cryptoxanthin	N	39.63±1.55 e	0.985	11.36±0.19 g	0.993	4.42±0.22 f	0.979	1.08±0.03 f,d,e	0.983
k_2	D	46.01±1.16 f	0.994	13.09±0.30 h	0.988	7.11±0.22 g,k	0.994	1.23±0.03 g	0.992
	J	32.78±0.30 g,b	0.997	10.54±0.34 i	0.977	8.71±0.45 h	0.981	1.24±0.04 h,l,m	0.980
F. (9*Z*/9'*Z*)-lutein	N	8.78±0.05 h	0.998	4.23±0.07 j	0.995	0.55±0.01 i	0.995	0.06±0.01 i	0.975
k_3	D	10.43±0.29 i	0.983	2.99±0.05 k	0.995	0.48±0.01 j	0.989	0.07±0.00 i,j	0.995
	J	13.17±0.37 j	0.984	2.50±0.02 l	0.997	0.56±0.01 i	0.998	0.08±0.00 j	0.995
D. (9*Z*/9'*Z*)-lutein	N	70.06±0.56 k	0.998	44.90±1.01 m	0.995	6.88±0.17 k	0.995	0.84±0.15 k,b,f	0.975
k_4	D	115.20±3.73 l	0.983	31.28±0.08 n	0.995	5.73±0.13 l	0.989	1.35±0.06 l	0.995
	J	126.49±4.40 m	0.984	31.05±0.28 n	0.997	5.34±0.07 m	0.998	1.28±0.10 m,g	0.995
F. (13*Z*/13'*Z*)-lutein	N	15.99±0.29 n	0.999	0.68±0.02 o	0.989	1.81±0.12 n	0.983	0.32±0.00 n	0.988
k_5	D	15.05±1.03 n	0.968	3.80±0.06 p	0.995	2.71±0.05 o	0.998	0.60±0.01 o,b,k	0.992
	J	18.67±0.60 o	0.992	4.39±0.03 q	0.998	2.82±0.01 o	0.991	0.73±0.02 p,k	0.990
D. (13*Z*/13'*Z*)-lutein	N	181.39±3.35 p	0.999	8.53±0.22 r	0.989	23.34±1.55 p	0.983	4.74±0.10 q	0.988
k_6	D	212.64±16.05 q	0.968	60.68±1.14 s	0.995	36.71±0.69 q	0.998	9.81±0.23 r	0.992
	J	273.69±9.80 r	0.992	66.71±0.49 t	0.998	34.64±1.32 q	0.991	12.27±0.32 s	0.990

[a] Reactions according to the kinetic mechanism showed in **Figures** 1 and 2. D, degradation; F, formation.

[b] S, Sample codex as in **Table** 1.

[c] Values are obtained from a minimum of 16 experimental data points analyzed in duplicate, SE, standard error; At each temperature, different l between rows indicate significant differences ($p \leq 0.05$).

Table 3. Analysis of Variance between the Rate Constant for the Total Degradation of Lutein (k_{tc}) and the Sum of the Rate Constants for the Individual Formation Reactions, (9*Z*/9'*Z*)-lutein (k_3) and (13*Z*/13'*Z*)-lutein (k_5) by t-test of Brown & Forsythe, 1974).

T (ºC)	S[a]	$[(k_3 + k_5) \pm SE^b] \times 10^3$ (h^{-1})	$(k_{tc} \pm SE^b) \times 10^3$ (h^{-1})
120	N	24.77 ± 0.30	25.44 ± 1.11
	D	25.48 ± 1.07	25.70 ± 1.68
	J	31.84 ± 0.70	32.17 ± 1.38
100	N	4.91 ± 0.07	4.94 ± 0.25
	D	6.79 ± 0.08	6.87 ± 0.36
	J[c]	6.88 ± 0.03	8.78 ± 0.29
80	N	2.36 ± 0.12	2.36 ± 0.13
	D[c]	3.19 ± 0.05	3.40 ± 0.12
	J[c]	3.37 ± 0.10	3.98 ± 0.14
60	N[c]	0.38 ± 0.01	0.44 ± 0.02
	D	0.66 ± 0.01	0.64 ± 0.03
	J	0.80 ± 0.02	0.77 ± 0.71

[a] S, Sample codex as in **Table 1**.
[b] SE, standard error. [c]Significant differences ($p \leq 0.05$) between $(k_3 + k_5)$ and k_{tc}.

Table 4. Thermodynamic Parameters[a] for the Thermal Degradation Reactions of Lutein and isomers, β-Carotene and β-Cryptoxanthin in Virgin Olive Oil.

Reaction[b]	S[c]	$\Delta S^{\#}$ ± SE[d] (cal/mol·K)	$\Delta H^{\#}$ ± SE[d] (kcal/mol)	Ea ± SE[d] (kcal/mol)	$\Delta G^{\#}_{298}$ ± SE[d] (kcal/mol)
D. *trans*-Lutein	N	-41.66 ± 2.46	16.11 ± 0.89	17.95 ± 0.24*[e]	28.53 ± 0.89
D. *trans*-Lutein	D	-45.14 ± 2.07	14.66 ± 0.75	16.27 ± 0.17	28.11 ± 0.75
D. *trans*-Lutein	J	-44.09 ± 1.77	14.89 ± 0.64	16.58 ± 0.14	28.03 ± 0.64
F. (9Z/9'Z)-lutein	N	-28.85 ± 3.56	21.58 ± 1.29	14.77 ± 0.31*	30.18 ± 1.29
F. (9Z/9'Z)-lutein	D	-29.51 ± 1.17	21.38 ± 0.42	12.20 ± 0.46	30.17 ± 0.42
F. (9Z/9'Z)-lutein	J	-29.23 ± 0.85	21.43 ± 0.31	12.43 ± 0.64	30.14 ± 0.31
D. (9Z/9'Z)-lutein	N	-30.73 ± 4.16	19.18 ± 1.50	19.70 ± 0.86	28.34 ± 1.50
D. (9Z/9'Z)-lutein	D	-31.43 ± 0.96	18.85 ± 0.35	20.63 ± 0.07	28.22 ± 0.35
D. (9Z/9'Z)-lutein	J	-29.73 ± 1.24	19.47 ± 0.45	21.02 ± 0.03*	28.33 ± 0.45
F. (13Z/13'Z)-lutein	N	-51.59 ± 9.98	13.06 ± 3.61	17.02 ± 0.67*	28.43 ± 3.61
F. (13Z/13'Z)-lutein	D	-52.29 ± 2.86	12.33 ± 1.03	13.86 ± 0.34	27.91 ± 1.03
F. (13Z/13'Z)-lutein	J	-51.48 ± 2.61	12.51 ± 0.94	14.11 ± 0.35	27.86 ± 0.94
D. (13Z/13'Z)-lutein	N	-49.50 ± 9.82	11.99 ± 3.55	15.29 ± 0.75*	26.74 ± 3.55
D. (13Z/13'Z)-lutein	D	-48.00 ± 2.06	11.94 ± 0.74	13.62 ± 0.27	26.25 ± 0.74
D. (13Z/13'Z)-lutein	J	-47.06 ± 2.22	12.19 ± 0.80	13.40 ± 0.36	26.21 ± 0.80
D. β-Cryptoxanthin	N	-44.50 ± 1.02	14.58 ± 0.37	15.93 ± 0.12*	27.84 ± 0.37
D. β-Cryptoxanthin	D	-44.89 ± 2.43	14.28 ± 0.88	16.60 ± 0.18*	27.66 ± 0.88
D. β-Cryptoxanthin	J	-50.20 ± 3.90*	12.42 ± 1.41*	15.15 ± 0.39*	27.38 ± 1.41
D. β-Carotene	N	-46.81 ± 0.59	13.83 ± 0.21	14.77 ± 0.06	27.77 ± 0.21
D. β-Carotene	D	-47.41 ± 0.85	13.67 ± 0.31	14.67 ± 0.14	27.80 ± 0.31
D. β-Carotene	J	-49.42 ± 0.31*	12.92 ± 0.11	14.30 ± 0.04*	27.65 ± 0.11

[a] $\Delta S^{\#}$, activation entropy; $\Delta H^{\#}$, activation enthalpy; Ea, activation energy, $\Delta G^{\#}$, Gibbs free energy.
[b] Reactions according to the kinetic mechanism showed in **Figures** 1 and 2; D, degradation; F, formation.
[c] S, Sample codex as in **Table** 1.
[d] SE, standard error.
[e] * Indicates significant differences for a parameter between different samples ($p \leq 0.05$).

Table 5. Isokinetic Temperature (T_{isok}) and Determination Coefficients (R^2) Estimated by Leffer´s Compensation Law ($\Delta H^{\#}_i = \Delta H^{\#}_0 + \beta \Delta S^{\#}$) for the Thermal Degradation Reactions of Carotenoid Compounds in Virgin Olive Oil.

Reaction [a]	**β** [c]	**SE**	**R^2**
D. *(E)*-Lutein	432.8	78.4	0.98
F. (9*Z*/9'*Z*)-lutein	316.8	68.9	0.96
F. (13*Z*/13'*Z*)-lutein	522.4	693.3	0.36
D. (9*Z*/9'*Z*)-lutein	71.3	80.4[d]*	0.44
D. (13*Z*/13'*Z*)-lutein	359.6	50.2	0.98
D. β-Carotene	371.8	27.7	0.99
D. β-Cryptoxanthin	366.7	24.8	0.99
Group of reactions [b]			
(9*Z*/9'*Z*)-lut and (13*Z*/13'*Z*)-lut isomerization reactions	390.8	7.9*	1.00
(9*Z*/9'*Z*)-lut and (13*Z*/13'*Z*)-lut degradation reactions	403.8	13.9*	1.00
Lut, β-carot and β-crypto degradation reactions	401.6	23.9*	0.98

[a] Reactions according to the kinetic mechanism showed in **Figures** 2 and 3; D, degradation; F, formation.
[b] Group of reactions; Lut, lutein; Carot, β-carotene; Crypto, β-cryptoxanthin.
[c] $\beta = T_{isok}$
[d] *Indicates significant differences ($p \leq 0.05$) with the mean harmonic temperature (T_{hm}) = 362K.